

PUDDLE POND RESOURCES LIMITED

---

Processing and Interpretation of IP/Resistivity Data  
collected on the Heritage Project,  
Burin Peninsula, Newfoundland and Labrador

**Peter Diorio P.Ge., GeophysicsOne Inc.**  
**22 July 2015**

FOR PUDDLE POND RESOURCES LIMITED

**GEOPHYSICSONE**<sup>INC.</sup>

---

## Table of Contents

Summary .....	3
Background .....	4
Regional Geologic Setting .....	4
Project Scale Geology.....	5
Terrain and Survey Conditions.....	7
Geophysics of Epithermal Gold Deposits .....	7
Data Sets and Processing .....	8
IP Data .....	8
Mag Data.....	8
Data Processing.....	9
Depth of Investigation .....	12
Data Presentation .....	12
Interpretation .....	13
Discussion of Anomalous Zones.....	14
Conclusions and Recommendations.....	20
References .....	22
Appendix 1 – Delivered data.....	23

## Summary

The main purpose of this work is to process and interpret data from a small (~20 line-km) 25m separation, dipole-dipole (Dp-Dp) Induced Polarization (IP) and Resistivity survey collected over part of the Heritage Project located on the Burin Peninsula in southern Newfoundland. The area is the site of a newly discovered low sulfidation epithermal gold-silver prospect which is currently being explored by Puddle Pond Resources Limited (PPR).

The data considered here includes approximately 10 km of IP collected in 2014 plus approximately 10 km of IP collected in early July 2015. The 2015 data includes extensions to the previous lines along with several additional lines. This report extends and essentially replaces a similar report (Diorio, 2014) which covered just the 2014 data.

Unconstrained 2D models of the *measured* IP and resistivity data were calculated using off the shelf 2D inversion software to produce *models* of the resistivity and chargeability. These replace the conventional pseudosections and, among other things, present the result with a true depth scale. Models were evaluated and depth of investigation was determined to be approximately 60 to 80m. Sections were prepared for resistivity and chargeability for each survey line and these were then used to construct level plans of both parameters at four horizontal slices at various depths below surface.

Data was integrated with geology and drill results provided by PPR. One of the most interesting anomalies closely follows the main mineralized zone known as the Eagle Zone. This suggests a strong empirical correlation between chargeability and this mineralized zone, probably due to pyrite or other sulfides spatially related with Au-Ag mineralization, though this remains to be confirmed. Many anomalous chargeability zones have been identified and are discussed in this report and most appear to present potential for further follow-up.

## Background

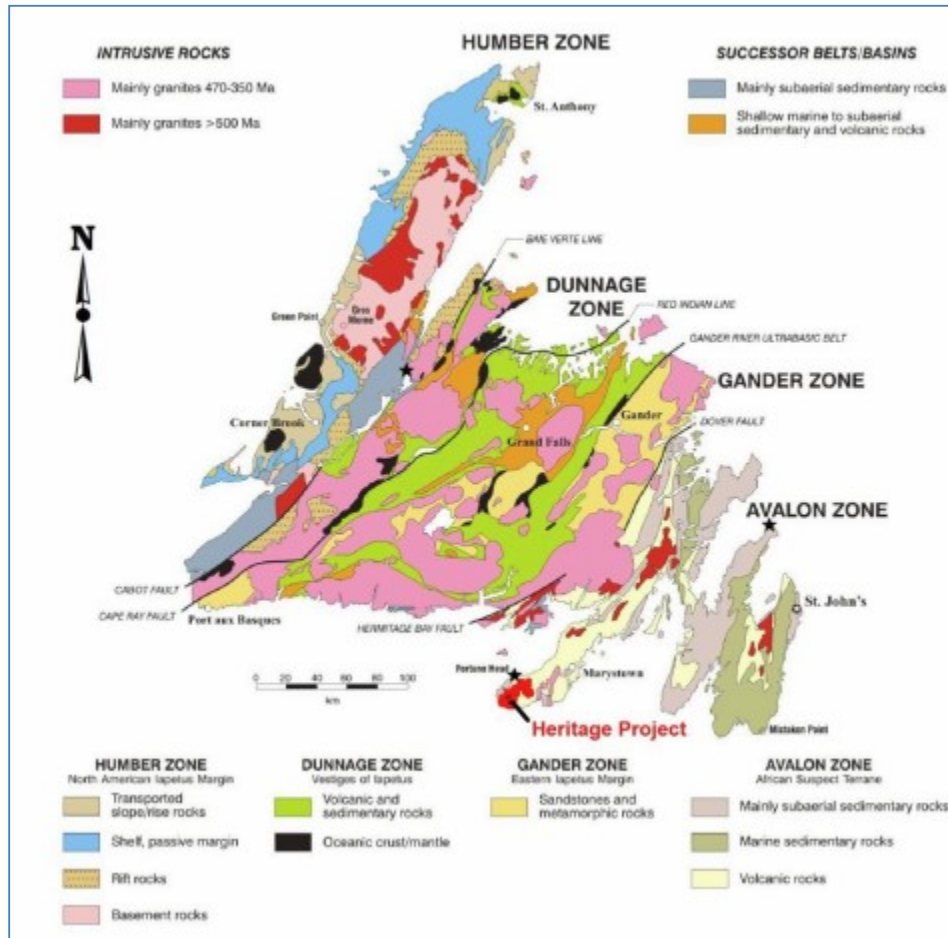


Figure 1 Project location on geology map of Newfoundland.

## Regional Geologic Setting

The project area (Figure 1) is located within the Avalon Zone, one of five tectonostratigraphic zones defined by Williams, 1979. The Avalon Zone is the result of the accretion of the Avalonia microcontinent to the Laurentia paleo-continent during the period 450 to 350 Ma (van Staal, 2007). The Burin Peninsula is located in the western margin of the Avalon Zone and has undergone several periods of deformation with the intensity of deformation broadly increasing from east to west. The structural history of the area is complex, the major deformational event(s) produced a series of open, isoclinal and recumbent folds with northwest dipping, shallow to steep axial planar schistosity. Vertical, transverse and thrust faults are common throughout the area.

## Project Scale Geology

The most recent available mapping in the immediate vicinity of the IP survey grid is extracted from the Woodlands, 2013 as shown in Figures 2 and 3.

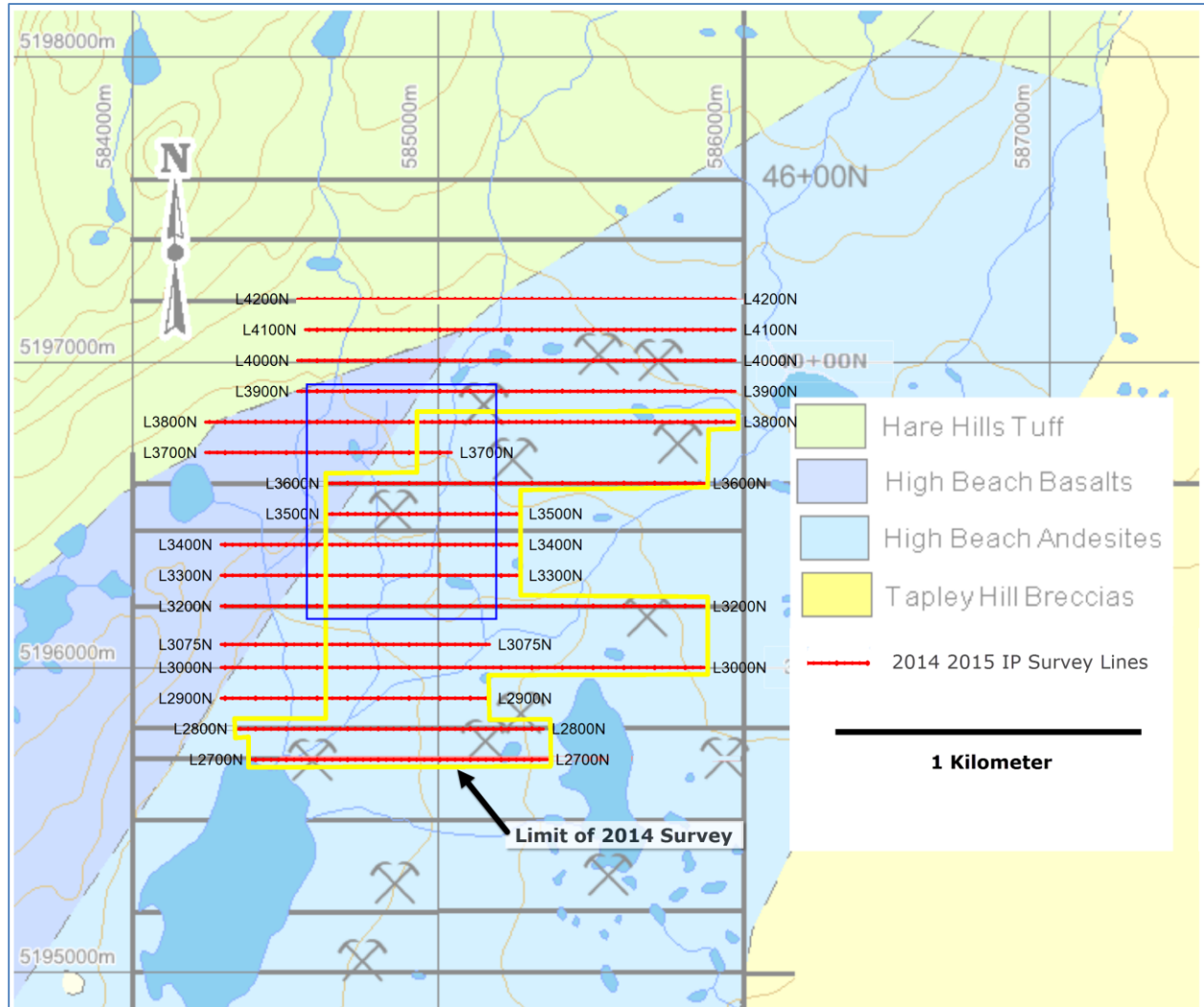


Figure 2 Location of 2014-2015 IP/resistivity survey lines (red) on project scale geology from Woodlands 2013. The line segments covered in 2014 are enclosed by the yellow polygon. The blue rectangle shows the limit of detailed geology shown in Figures 3.

The area north and west of the IP survey grid is principally underlain by the Hare Hills Tuff (HHT) comprised of felsic volcanics. The High Beach Basalts (HBB), which contacts the HHT along its southeast margin, is composed of a flow and tuff member as well as a red micaceous sandstone and conglomerate, representative of a volcanic arc type environment. The 2012 mapping outlined the newly recognized High Beach Andesite unit (HBA) to be a distinct lithologic unit which appears to be the exclusive host to the extensive epithermal alteration system of the Point May Epithermal System (PMES). The HBA

contains two members consisting of an andesite porphyry flow and a poorly sorted lithic tuff, indicative of a volcanic arc environment. Epidotization and saussuritization of the plagioclase and clasts of the HHA is due to a regional low-grade green schist metamorphism common throughout the area. (Woodlands, 2013)

While the 2014 survey was almost completely limited to the HBA the survey lines completed in 2015 extend the coverage to the north and west into the HBB and HHT as shown in Figure 2.

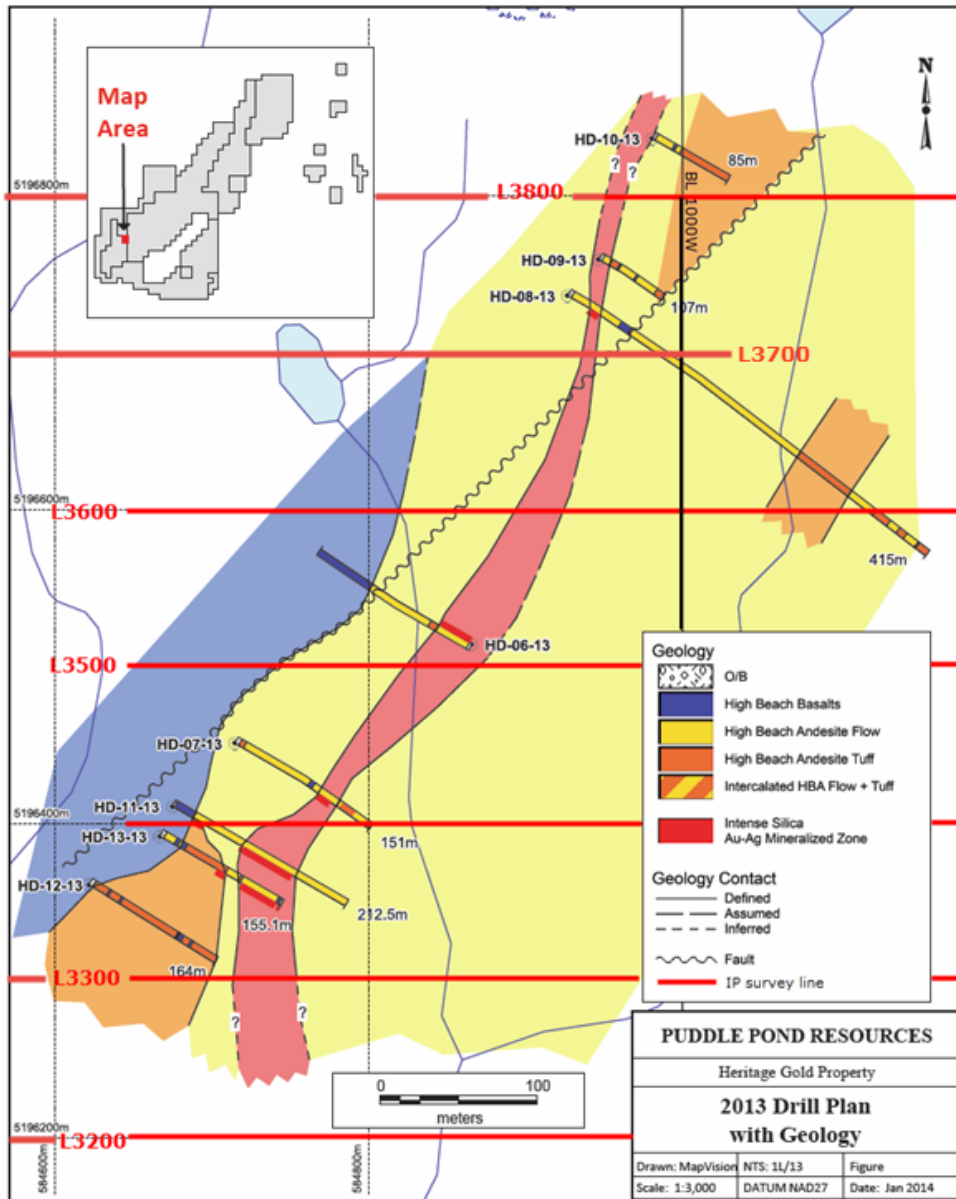


Figure 3 Detailed geology and drilling in the Eagle Zone, located in the central part of the IP coverage (After Woodlands, 2013) See Figure 2 for location.

## **Terrain and Survey Conditions**

The terrain on the Heritage Project is characterized as an extensive plateau area of wet, marshy to dry barrens punctuated by small hills and north-south trending, gentle ridges, typical of the landscape in this region. Outcrop is very sparse throughout the Heritage Project, essentially restricted to the hilltops and ridges, with rare exposures along some of the major streams and smaller, intermittent streams that drain the area. The low-lying areas, both wet and dry, appear to be covered by a widespread blanket of till and overlying soils, which exposed during the trenching, ranges in thickness generally between less than 0.5 and 2-3 metres. (Woodlands, 2013). Thin uniform till presents favorable environment of for IP surveys since it provides a suitable medium for making electrical contact with the ground without significant conductive cover which can mask the response from bedrock.

## **Geophysics of Epithermal Gold Deposits**

Epithermal gold deposits are highly variable in form, ranging from thin quartz veins to large disseminated deposits, and are located in a variety of geological environments. Consequently, they exhibit a wide range of geophysical signatures. Hydrothermal alteration accompanying these deposits causes pronounced changes in the physical properties of the rocks. Magnetic susceptibility and remanence decrease due to the destruction of magnetite; the potassium content commonly increases causing an increase in radioactivity; the electrical resistivity changes by up to two orders of magnitude; and the density increases or decreases depending on the nature of the host rock and alteration processes (Irvine and Smith, 1990). Pertinent to the IP/resistivity data considered here we may expect resistivity to either decrease dramatically due to the replacement of feldspars by clay or, conversely, it may increase dramatically due the introduction of silica. Parts of the system may be dominated by pyrite, or in some case base metal sulfides, and these can be expected to produce significant chargeability anomalies. While these will be the main focus of the investigation here the correlation between pyrite or other sulfides and Au/Ag mineralization is not clear, so this must be kept in mind when using this data for interpretation and targeting.

## Data Sets and Processing

### IP Data

The IP survey data discussed here was acquired in May 2014 and July 2015 by Eastern Geophysics using a Phoenix IPT1 transmitter and Iris Lrec Pro receiver. Approximately 18.8 km<sup>1</sup> (16 lines) of time domain, dipole-dipole, and IP / Resistivity data collected using a dipole length of 25m and N separations of 1 through 6 are the focus of the work here. The IP/Resistivity data cover an area extending approximately 1.5km (N-S) and 1.8 km (E-W) (Figure 2). Details of the operation are covered in the Eastern Geophysics 2014 and 2015 logistics reports and are not covered again here.

Current levels were consistently high with a mean of .45 amps and a range from .12 to 1.10 amps. Such levels are adequate to generate useful signal levels for IP measurements given the thin overburden and typically high resistivity of the local geology. Measured primary voltages were typically about .75 volts and ranged from 5.3 mV to almost 10 volts. In two instances voltage saturation at the shortest N separation may be problematic.

Data was loaded into Geosoft and each IP decay curve was inspected for obvious deviations from a typical smoothly decaying voltage.

In general the quality appears to be very good and only extremely rare spurious events were noted and deleted.

### Mag Data

Mag data was provided only as a colored image without color bar or contours (Figure 4) so anomaly amplitudes are not known. Processing the mag data is not part of this work and the mag data is not integrated into this interpretation.

---

<sup>1</sup> This is the end-to-end length of the survey coverage and excludes approximately 175m of overlap on each line that was extended during the 2015 survey



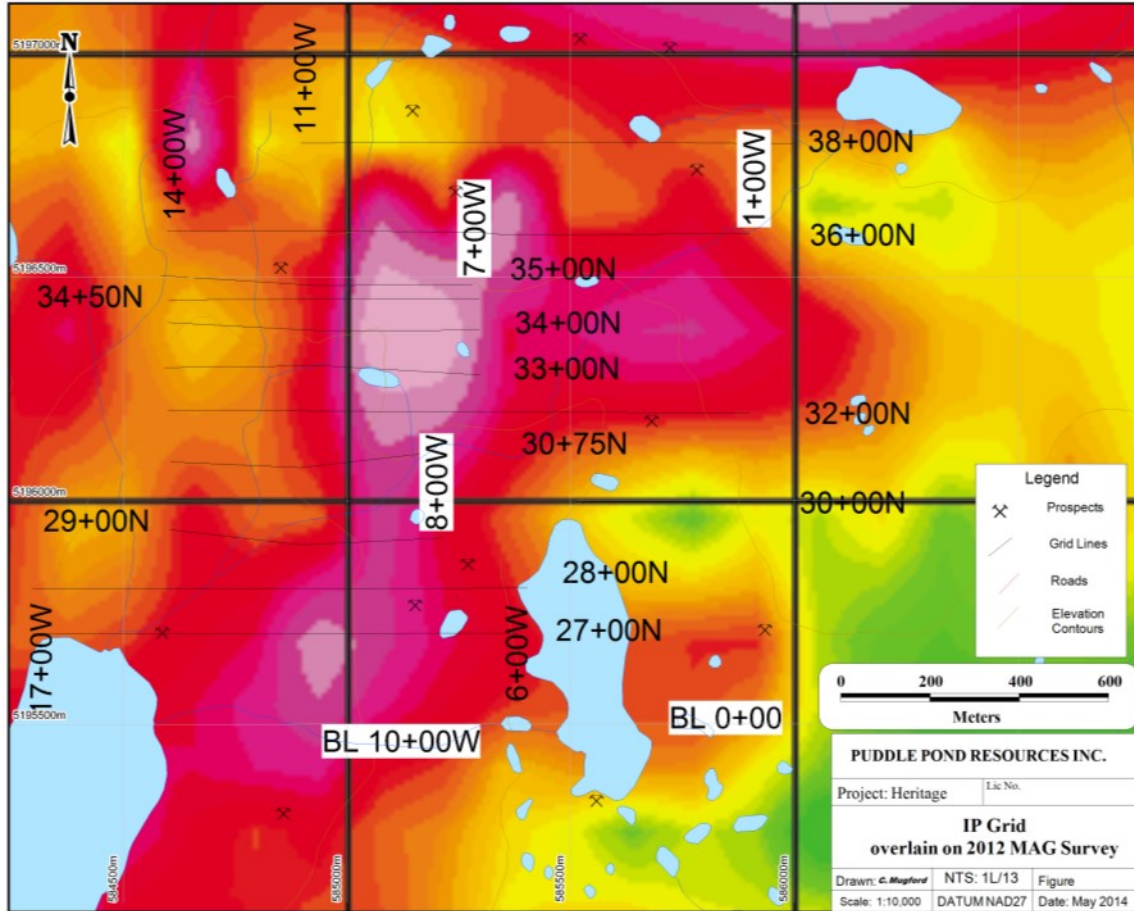


Figure 4 Mag data, as supplied.

## Data Processing

**Geophysical Inversion** is a process that takes any set of geophysical observations collected on the surface or in the air (in this case *voltages* and *apparent chargeability* traditionally displayed as pseudosections) and determines a distribution of the physical parameters within the earth which could give rise to those measurements (in this case *modeled* resistivity and *modeled* chargeability). See Figure 6. By this process factors such as topography (if available), geometric effects inherent in the electrode array and the effect of non-uniform resistivity are taken in to account. This permits the measured *apparently* chargeability and *apparent* resistivity (which traditionally are displayed with only “N” separation as the vertical scale) to be replaced by *modeled* resistivity and chargeability which are generated at true vertical depth (Figure 6). The result, while still an approximate model due to a number of limitations, is generally much more directly comparable to drill results than conventional pseudosections.

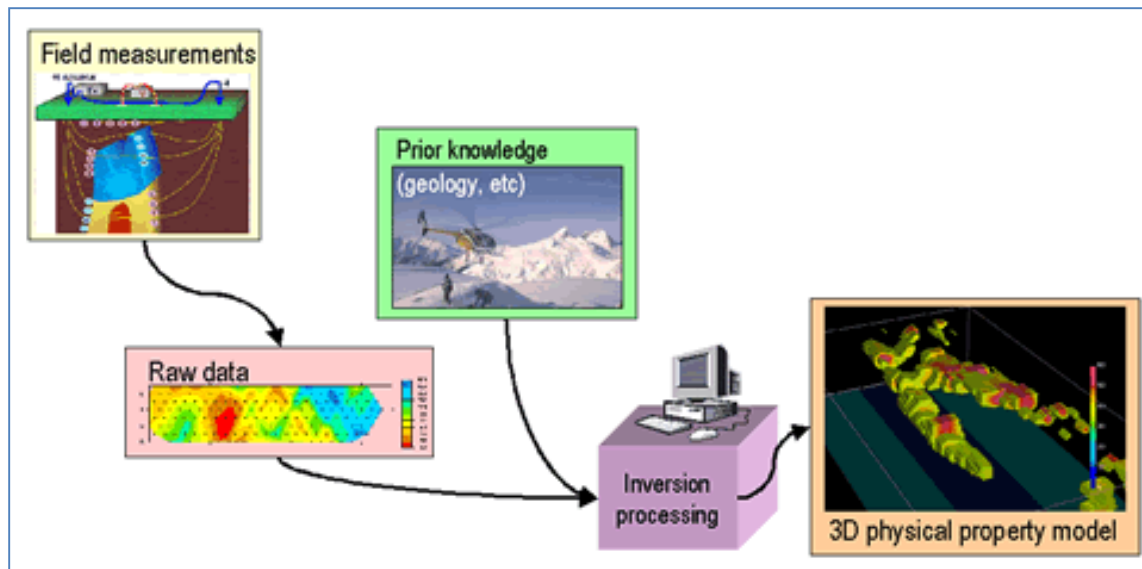


Figure 5 Thematic representation of Inversion process.

The inversions completed here are unconstrained<sup>2</sup> 2D inversions for each line of IP and Resistivity data and produce a series of 2D model cross sections of the earth. These in turn were used to construct level plans (i.e. depth slices) extracted at various depths for each of the two parameters.

Models of this sort are inherently non-unique which means that many different models could fit the data to the same level of accuracy and it can be demonstrated that if the models are allowed to be arbitrarily complex then an infinite number of such models can be created. However many of these models will be unjustifiably complex and geologically or physically unrealistic. This dilemma is avoided by forcing the model to be in some defined sense the *simplest* model that fits the data. In this case we define the *simplest model* as the mathematically smoothest model. Such a model is unique however it is worth noting that many geologic contacts are relatively sharp so forcing the model to be smooth across such boundaries carries its own set of limitations.

---

<sup>2</sup> Unconstrained inversion does not impose a priori geologic constraints on the model.

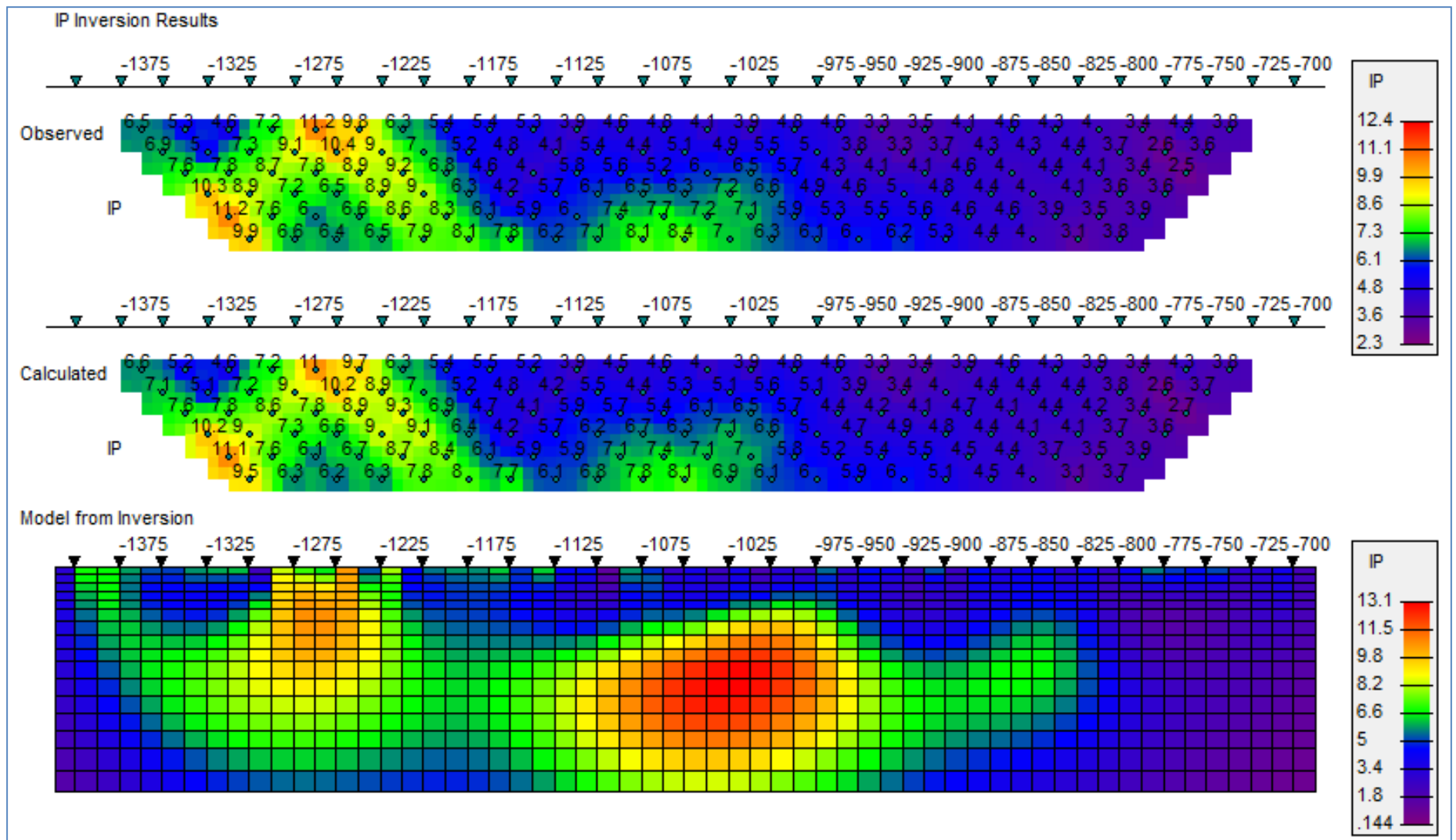


Figure 6 Chargeability inversion for L3300N. Top panel shows the measured data in pseudosection form. The bottom panel shows the inverted section. The middle panel shows the pseudosection data calculated from the model. The results illustrate that although the highest measured amplitudes are observed over the shallow anomaly at about -1275 a significantly stronger anomaly is responsible for the deeper source located near the centre of the section.

## Depth of Investigation

The depth of investigation (DOI) of the survey and resulting chargeability model can be challenging to estimate. Here the DOI is determined following the method of Oldenburg and Li, 1997. Each chargeability inversion was computed twice. The first run used a starting and reference<sup>3</sup> model which is essentially zero, representative of benign, background geology without any significant chargeability. The second run used a starting and reference model with a large uniform chargeability, in this case 50mV/V. Where the two resulting inverted models are nearly identical the result is heavily influenced by the measured data and we can have high confidence in the result. However, where the models differ significantly then we have lower confidence in the model because the result is dominated by initial, arbitrary conditions (i.e. the starting and reference models) and not by the data. On the model sections a dashed yellow line shows the depth at which difference between the two model runs is 10% of the anomalous reference model (Figure 7). In the central part of the sections this is at a depth of 75m or so and is shallower towards the ends of each line where the measured data coverage is incomplete. This should not be treated as a hard and fast line of demarcation instead it should be used as a guideline with the model being more reliable above the line and less reliable below it.

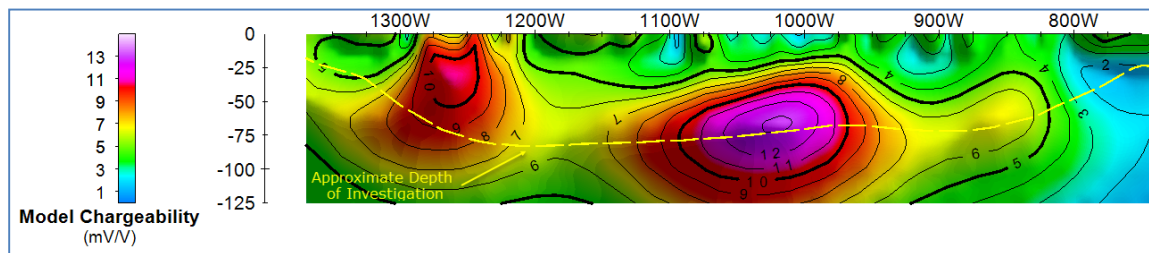


Figure 7 Chargeability model for Line3300N. The dashed yellow line indicates the approximate depth of investigation.

## Data Presentation

All data is presented as sections (e.g. Figure 7) and plans for both the chargeability model and resistivity model at various depths from 28m to 80m below surface (e.g. Figure 8 and 9). All the chargeability plans and sections use an identical linear color stretch from 0 to 16 mV/V. All the Resistivity plans and sections use an identical non-linear color stretch which has an equal area colour distribution for a plan constructed at a depth of 44m, approximately through middle of the models.

---

<sup>3</sup> The “reference model” is used in the modelling process to influence those areas which are not well constrained by the available data, for example deep regions or regions off the ends of the coverage. It is usually set to a non-anomalous value (~0 in the case of chargeability) so the resulting inversion model will smoothly relax to this value rather than drifting into uncontrolled anomalous levels. The “starting model” is simply the initial guess that the iterative process commences with.

All results here use idealized local coordinates.

## Interpretation

Anomalous regions from the resistivity and chargeability plans and sections have been compiled on to an interpretative layer as shown in Figures 8 and 9 and on the accompanying 1:5000 plan maps. With the addition of new data in 2015 the shape and intensity of some of the anomalies have changed and several new anomalies have been added, some of which are quite strong. Weak to moderate amplitude chargeability anomalies are marked with a cyan hachure pattern and the higher chargeability anomalies are marked with solid cyan polygons on the interpretation plans. High resistivity zones are marked with a black stipple pattern. These polygons, while useful to highlight anomalous regions, are diagrammatic and mask some of the complexity of the chargeability and resistivity responses. See discussion in Diorio 2014. The reader is directed to the appended sections for details of each survey line.

**NOTE** the anomaly annotations have been changed, when necessary, so the reader should not expect exact correspondence between anomaly labels used in Diorio, 2014 and those used in this report.

The chargeability anomalies in this survey are generally associated with regions of low to modest resistivity (e.g. Zones A1, A2, C, F1, F2 and part of B) while the southern part of Zone B and all of Zones G1, G2, G3, H1, H2, J1 and J2 correlate to areas of high resistivity. These areas of high resistivity may reflect silicification (as well as other factors as discussed above) and low resistivity may reflect alteration to clay, extensive fault gouge or, perhaps less likely in this environment, sulfide mineralization or graphite. Although detailed topographic elevations were not available it is evident that streams pass *between* the regions of highest resistivity suggesting that thicker overburden in the lower-lying areas may be responsible for depressing the resistivity locally. Alternatively, these minor valleys may reflect the surface expressions of faults which have fractured the rock, with commensurate increase in permeability and porosity and thus lower resistivity. It is also likely that both thicker overburden and faulting contribute to the lower resistivity.

In overview, the resistivity is dominated by a large region through the central part of the survey area where the resistivity is rather high, generally in excess of 5000 ohm-m and up to 30,000 ohm-m or more (Figure 9). This appears to correlate quite well with the inner zone of adularia/chalcedony alteration from Woodlands, 2013 (see dashed outlined, Figure 9). The spatial correlation between the inner alteration zone and high resistivity is well defined along their western boundary but less clear to the east

where the extent of the IP/resistivity survey is too limited for this interpretation to determine if the high resistivity zone is limited to the inner alteration zone or may result from intrinsic high resistivity of the andesite tuffs / flows or simply might reflect widespread silicification. Field inspection or review of extant detailed mapping may be required to determine which interpretation is most appropriate. Physical property measurements on core or hand samples may also be helpful in determining this.

Both the High Beach Basalt and the part of the High Beach Andesite located to the east of the inner alteration zone exhibit much lower resistivity. The sheared/faulted contact between the HBB and HBA is mapped well by a narrow, linear moderate-to-high chargeability and low-resistivity feature (Zone F1 and possibly F2). The chargeability is variable along this zone and local highs may be of exploration interest. Note that one of these highs, centred on L3500N at 12+60W was previously lumped in Zone A (Diorio, 2014) but it has distinctive geophysical properties is now interpreted to reflect the fault zone as manifest in Zone F1.

The basalt, which generally has low resistivity, is punctuated by three zones of high resistivity and high chargeability (Zones G1, G2 and G3) each with dimensions approximately 50m x 200m. These may reflect localized alteration within the basalt.

## Discussion of Anomalous Zones

**Zone A1** is a zone of moderate to high chargeability with intermediate resistivity as shown in Figures 8 and 9. The zone closely coincides with Eagle silica Au-Ag mineralized zone (Figure 10). This is an important outcome since it seems to support a direct spatial correlation between this IP anomaly and Au-Ag mineralization. Given the erratic nature of the Au-Ag grades, even relatively small anomalies within Zone A should be carefully considered as potential targets.

**Zone A2** has similar characteristics to Zone A1 and may simply be its continuation to the north. Note that the highest *measured* (as opposed to *modelled*) chargeability observed in the entire survey occurs at the smallest N-separations at the eastern end of L3700N. This has two implications: firstly Zone A2 is open to the east on this line and secondly the modelled chargeability for A2 is almost certainly underestimated here since the unconstrained inversion will tend towards background values (as defined by the reference model) in areas where no data is available, including near the ends of lines.

**Zone B** appears to be largely untested and presents a number of interesting targets, notably small near-surface anomalies on line 3500N (possibly amenable to trenching) and deeper, larger anomalies

particularly on L3600N and 3300N. Hole HD-13-08 would have passed through the plane of this zone but at a depth of 150m or more, which is considerably deeper than the depth of investigation of the IP survey. Gold assays of less than 1 g/t over two short intervals are noted at approximately the expected plane of the Zone.

**Zone C** is similar in character to Zone E with a relatively modest chargeability anomaly coincident with a resistivity low at depth. HD- 13-05, located approximately 50m north of L2800N and targeted at “Turpins Trench#1” appears to have tested or partially tested Zone C. The cause of the anomaly is not clear on the available drill cross section and detail logs should be consulted to see if the cause can be determined. In any case, Zone C is strongest on line 3000N, about 150m north of HD-13-05 and on this line at 575W there is a small near-surface expression of the zone, possibly amenable to surface trenching. This site presents a high priority target.

**Zone D** represents zone of weak chargeability and high resistivity and should be evaluated in conjunction with the data from the nearby “Flatbed” prospect/showing and assessed accordingly.

**Zone E**, which in 2014 was limited by survey coverage to just lines 2700N and 2800N can now be traced for at least 500m and is open to the south. It may present a possible extension of Zone A, albeit somewhat deeper and with lower amplitude chargeability. As with Zone A the chargeability follows a zone of low to modest resistivity and so Zone E also presents a high priority target.

**Zone F1** is a narrow, linear, moderate to high amplitude chargeability and low resistivity feature which closely follows the sheared/faulted contacted between the HBB and the HBA. The chargeability is variable along this zone and local highs may be of exploration interest. Note that one of these local highs, centred on L3500N at 12+60W, was previously lumped in **Zone A** (Diorio, 2014) but it has distinctive geophysical properties is now designated **Zone F2**. It is interpreted to reflect a fault zone similar to Zone F1. If this interpretation is correct then the location of the fault needs to be revised in the vicinity of F2 or a fault splay added.

**Zones G1, G2 and G3** all occur within the HBB and all represent localized chargeability anomalies with coincident resistivity highs. They occur outside the currently defined limits of the PMES and related alteration (Figure 10) so they may be considered lower priority at this time however they are distinctly anomalous and localized so they should not be discounted completely until the cause of the anomalies is established.

**Zones H1 and H2** are large, high amplitude chargeability anomalies which arguably form just a single contiguous anomaly which is open to the north. The modelled chargeability is much higher than other anomalies within the survey area and it peaks on line 4100N at approximately 6+00W where modelled chargeability exceeds 38 mV/V. The anomalies are associated with moderately high resistivity of at least 5000 Ohm-m with H2 having higher resistivity than Zone H1. Zone H2 is located entirely within the HBA while Zone H1 straddles the mapped triple point boundary with the HBB to the west, HHT to the north and HBA to the east. The contacts are inferred in this vicinity and the accuracy of the mapped boundaries is uncertain.

The high chargeability as well as considerable lateral extent of Zones H1 and H2 are appealing and the first step is to try to establish if they arise simply from widespread pyritic alteration or are related to alteration which is more closely associated with gold mineralization.

**Zones J1 and J2** are moderately high amplitude chargeability anomalies related to local resistivity highs which occur peripheral to a large resistivity high centred between these zones and Zone D. Zones J1 and J2 both extend across the northern two lines of the survey coverage and are open to the north. They occur within the HBA in a geophysical setting similar to Zone D. Zone J1 is strongest on line 4200N about 200m north of the Whales Back Prospect (Woodland, 2013) which may provide some insights into the prospectivity of the zone.

Other spatially small anomalies are noted on the sections and these should be evaluated in concert with surface prospecting, trenching and geochemical data.



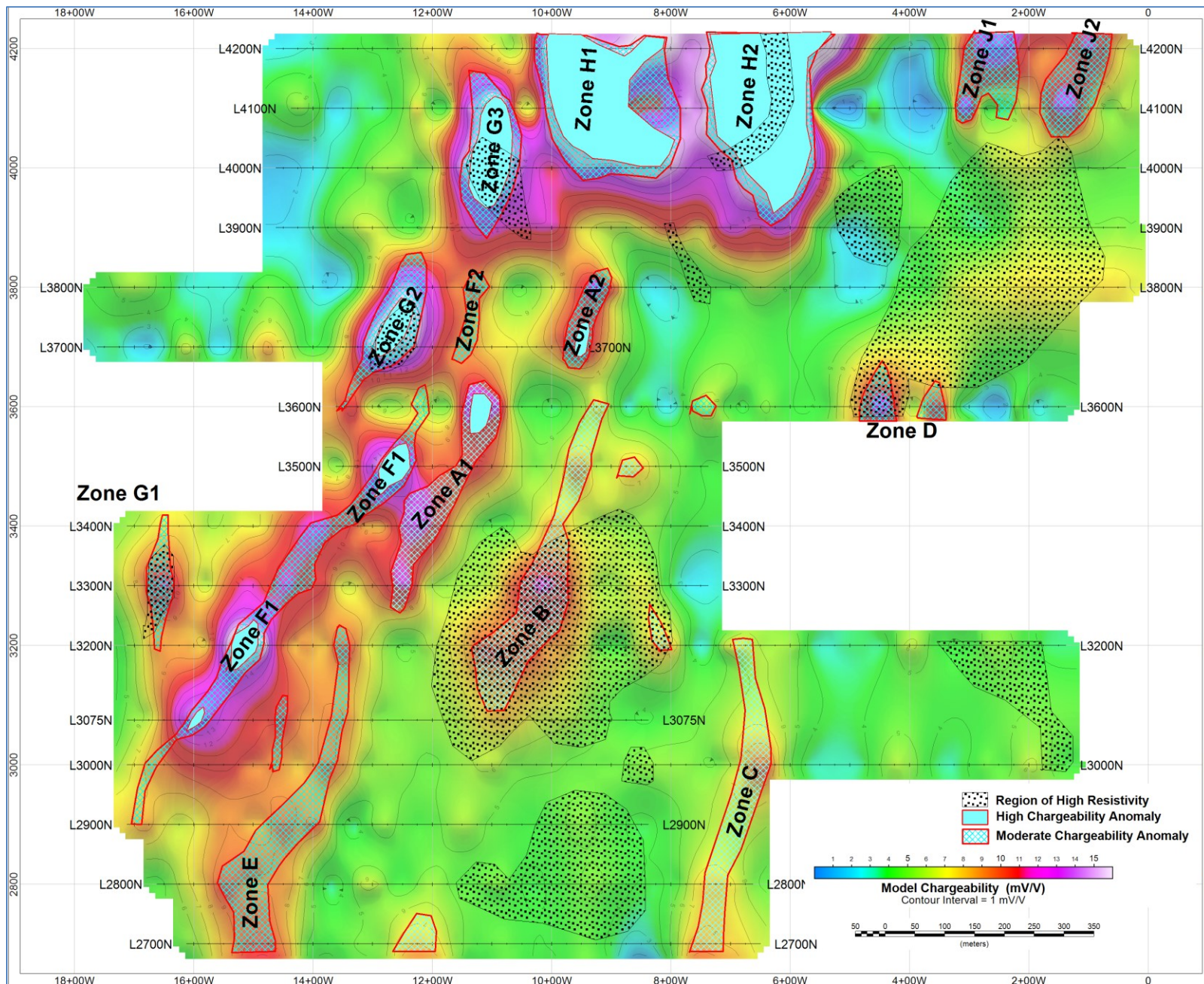


Figure 8 Interpreted anomalous chargeability and high resistivity zones on the 44m depth slice constructed from the 2D chargeability sections.

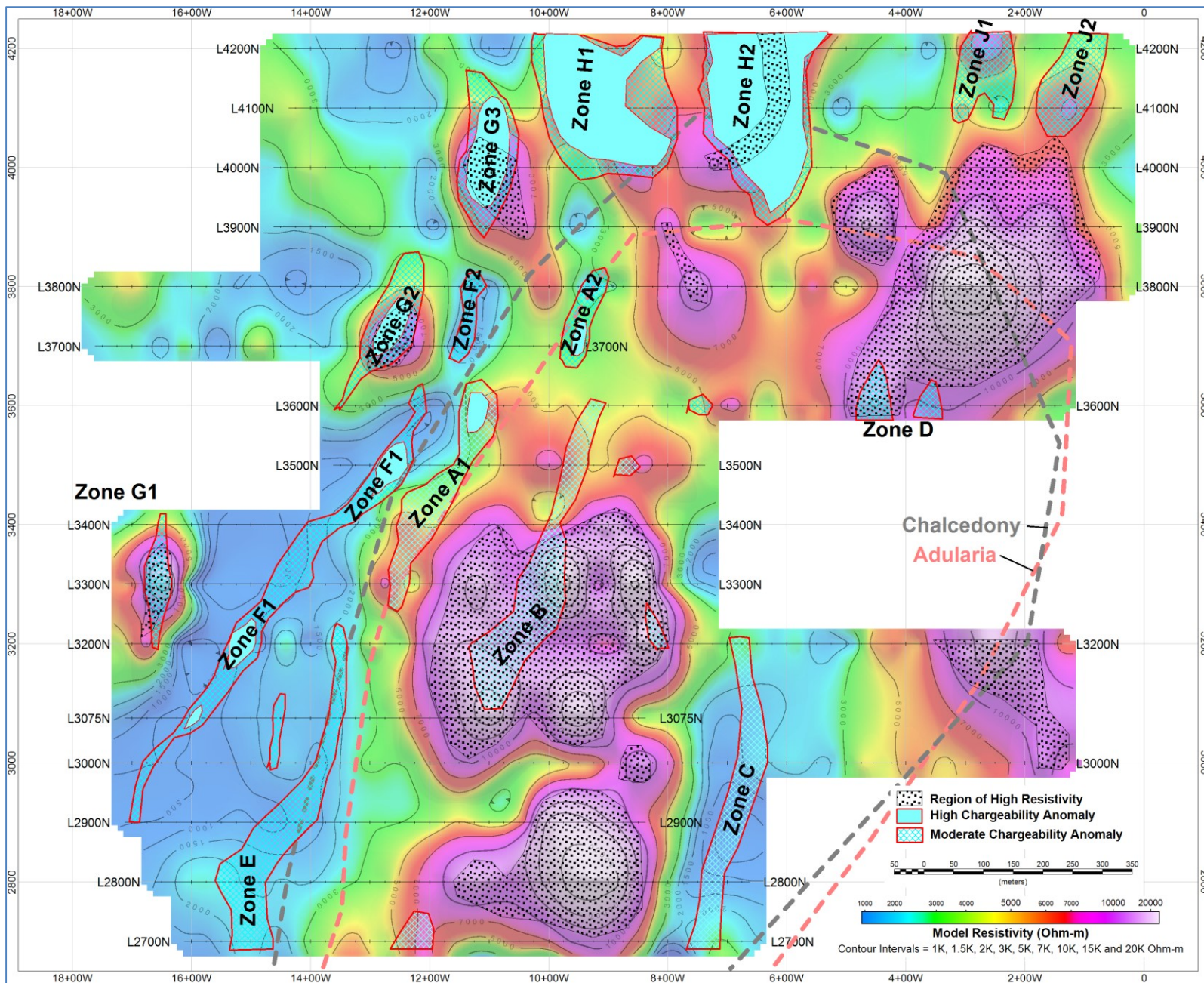


Figure 9 Interpreted anomalous chargeability and high resistivity zones on the 44m depth slice constructed from the resistivity models. The “inner” chalcedony and adularia alteration zones are shown as dashed lines.

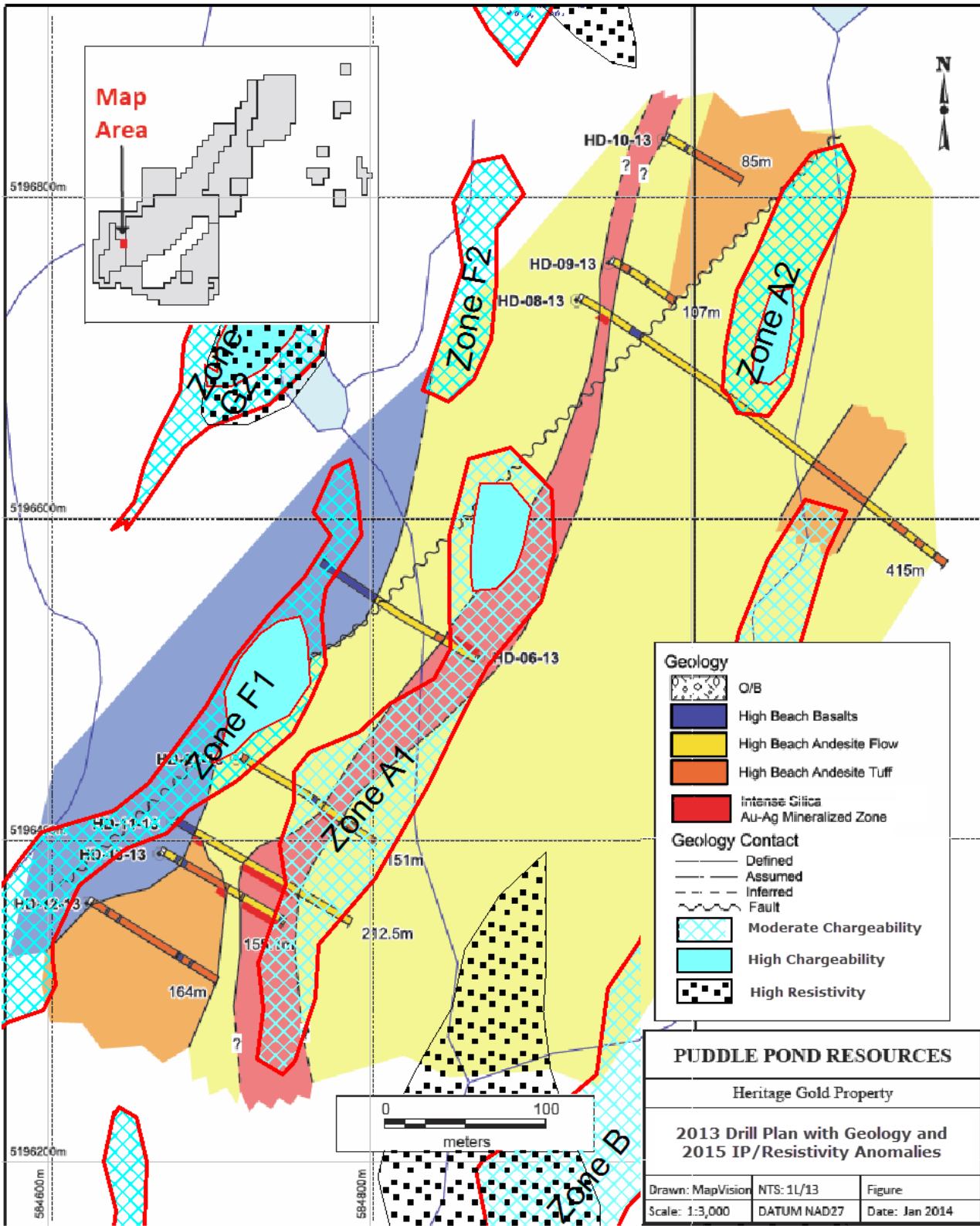


Figure 10 Chargeability anomalies overlain on detail geology in the Eagle Zone area.

## Conclusions and Recommendations

The IP survey data and resulting models successfully outlined several zones of anomalous chargeability and one of these zones correlates well with known mineralization in the Eagle Zone area. The cause of this is presumed to be sulfide mineralization associated with Au-Ag mineralization but this remains to be confirmed. That said, a large pyrite alteration zones (larger than the extent of the IP survey) is noted in Woodland 2013 and furthermore gold mineralization is not known to be related to pyrite concentration so this implies that IP and resistivity must be used cautiously and with careful consideration of all geoscience data.

- Conclusively establishing the cause of the IP and resistivity anomalies outlined herein remains the most important follow-up priority. Specifically, relating the IP/resistivity results to *mapped* and *drill determined* alteration data, rather than to the *extent of interpreted* alteration zones, should be a priority. Several of the anomalies within Zone A and possibly Zone B have been drill tested however the source of the chargeability anomalies has not been determined. This should be established using the detailed drill logs. Physical property measurements on core may also be helpful.
- Based on the interpretation and limited integration of the IP/resistivity results with other available exploration data which is presented here several zones appear to present highly attractive drill targets. Specific target selection should be assessed and revised by those more familiar with the local geology and exploration history than the writer.
- Zone F1 appears to closely map the fault-bounded contact between the Hare Hills Andesite and Hare Hills Basalt. Chargeability anomalies along this structure would seem to present high priority targets. Zone F2 has similar geophysical characteristics and therefore may trace the fault to the north with the obvious implication that the trace of the fault should be revised or a splay added to account for Zone F2.
- While the plan depth slices are very useful for interpretation it is recommended that sections be used for detailed definition of any drill holes so that the vertical dimension is taken into consideration. Attention should be paid to the depth of investigation (dashed yellow line on the Chargeability sections) since this gives a rough indication of the depth at which the sections become unreliable.
- Survey parameters used here seem appropriate for the target and local conditions. Although the IP coverage now seems largely complete for this part of the alteration system, follow-up extension

may be warranted in a few places. In particular the coverage of L3700N should be expanded to the east to close off the highest amplitude chargeability measured during the course of the survey. High amplitude modelled chargeability associated with Zones H1 and H2 should be followed up to the north of L4200 if these zones are found to be of exploration importance. A couple of long IP traverses (a=50m, N=1 to 4) across the PMES and extending outside it and would be useful to establish regional backgrounds.

- Mag data can often be very helpful in gold exploration if it is gathered with sufficient sample density. Mag data collected on 50m spaced lines (or less) with station spacing of not more than 5m is desirable.

Respectfully,

A handwritten signature in blue ink that reads "P. Diorio". The signature is fluid and cursive, with the first name "P." and the last name "Diorio" clearly legible.

Peter Diorio, P.Geol.  
GeophysicsOne Inc.

## References

**Carmichael, R .S., 1989**, Practical Handbook of Properties of Rocks and Minerals, CRC Press

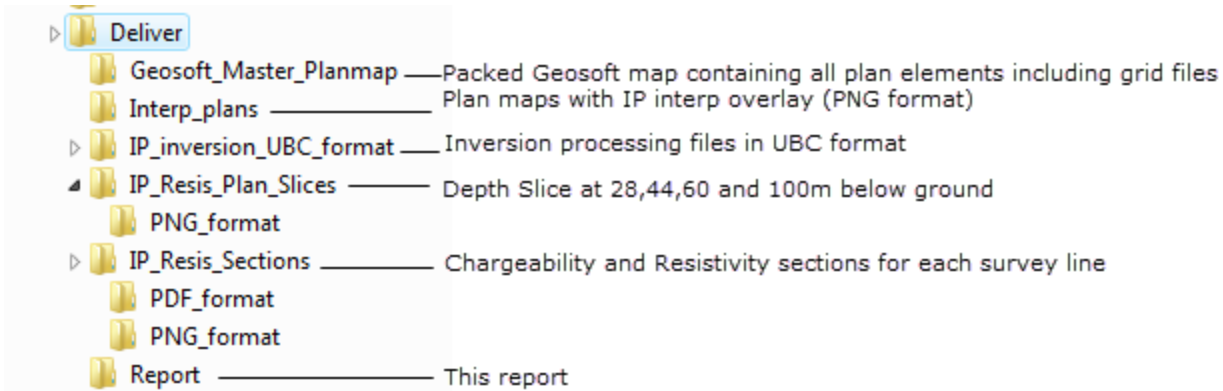
**Diorio, P.A., 2014**, Processing and Interpretation of IP/Resistivity Data collected on the Heritage Project, Burin Peninsula, Newfoundland and Labrador, Unpublished report for Puddle Pond Resources Inc.

**vanStaal, C., 2007**, Pre-Carboniferous Tectonic Evolution and Metallogeny of the Canadian Appalachians. In W. Goodfellow, Mineral Deposits of Canada: A Synthesis of Major Deposit

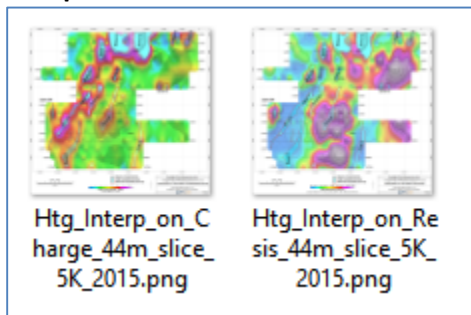
**Irvine,R.J. and Smith,M.J.**, Geophysical Exploration for Epithermal Gold deposits, Journal of Geochemical Exploration, Vol 36, Issues 1–3, February 1990

**Woodland,G., 2013**, Technical Report, Heritage Project, Burin Peninsula, Province of Newfoundland & Labrador, Canada, Unpublished report for Puddle Pond Resources Inc.

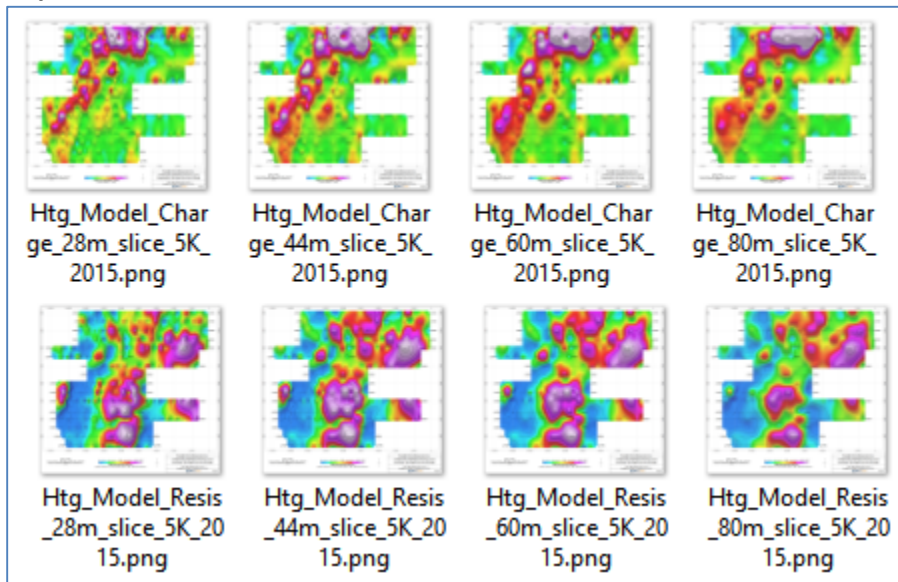
## Appendix 1 – Delivered data



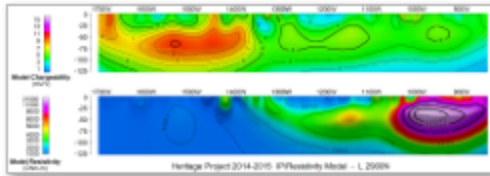
### Interpretation Plans



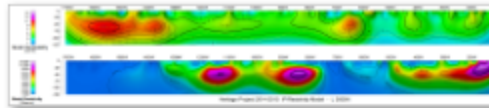
### Depth Slices



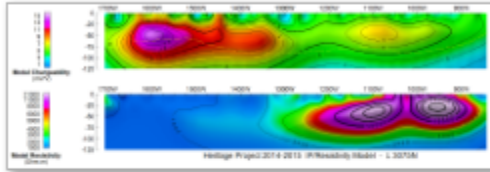
## Chargeability and Resistivity Sections



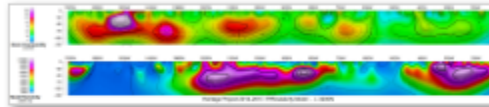
Htg\_Model\_IP\_Res\_section\_2015\_L2900N.png



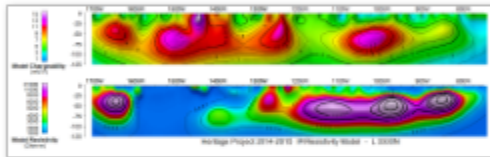
Htg\_Model\_IP\_Res\_section\_2015\_L3000N.png



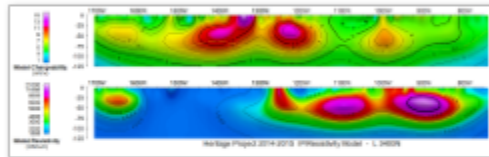
Htg\_Model\_IP\_Res\_section\_2015\_L3075N.png



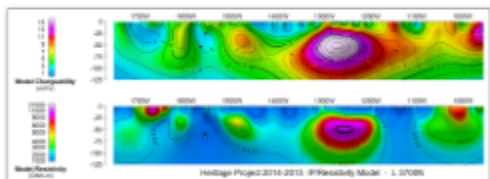
Htg\_Model\_IP\_Res\_section\_2015\_L3200N.png



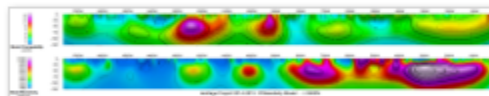
Htg\_Model\_IP\_Res\_section\_2015\_L3300N.png



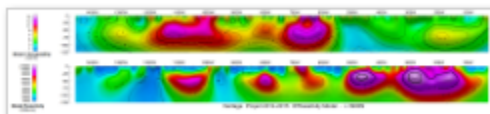
Htg\_Model\_IP\_Res\_section\_2015\_L3400N.png



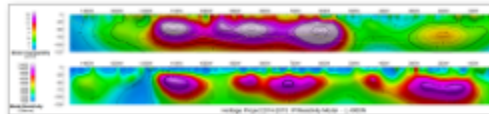
Htg\_Model\_IP\_Res\_section\_2015\_L3700N.png



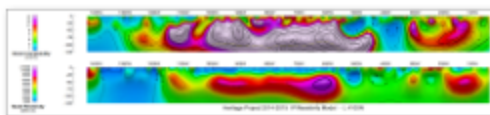
Htg\_Model\_IP\_Res\_section\_2015\_L3800N.png



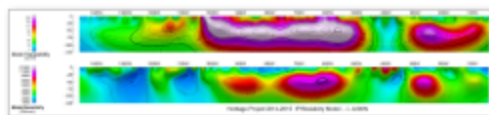
Htg\_Model\_IP\_Res\_section\_2015\_L3900N.png



Htg\_Model\_IP\_Res\_section\_2015\_L4000N.png



Htg\_Model\_IP\_Res\_section\_2015\_L4100N.png



Htg\_Model\_IP\_Res\_section\_2015\_L4200N.png